

# A VARIABLE-RATE FILTERING SYSTEM FOR DIGITAL COMMUNICATIONS

Larry Wasserman and Alan N. Willson, Jr.

Integrated Circuits and Systems Laboratory  
Department of Electrical Engineering  
University of California, Los Angeles  
Los Angeles, CA 90095  
larryw@icsl.ucla.edu, willson@icsl.ucla.edu

## ABSTRACT

We propose an efficient programmable transmit-receive digital filter structure consisting of a pulse-shaping filter (PSF) and a cascaded integrator-comb (CIC) filter which is applicable to variable-rate digital communication systems. The CIC structure is a hardware-efficient means of constructing programmable interpolation and decimation filters, but it introduces a large amount of inter-symbol interference (ISI). We solve this problem by proposing a filter design method that determines the PSF coefficients such that the cascade of the PSF and CIC filter exhibits the desired frequency response.

## 1. INTRODUCTION

Interpolation and decimation filters are important elements in digital communication systems. Fig. 1(a) shows a variable-rate digital modulator, and Fig. 1(b) shows the corresponding digital demodulator filter structure. In the modulator, the PSF bandlimits and shapes the signal to accommodate the band-limited channel and to achieve zero ISI, and the interpolation filter increases the sampling rate in accord with the difference between the symbol rate and the IF center frequency and attenuates the images due to the upsampling. In the demodulator, the decimation filter reduces the sampling rate and acts as the anti-aliasing filter for the downsampling, and the PSF completes the matched filter structure. In QAM systems, the cascade of the PSF and interpolation/decimation filter typically exhibits a square-root Nyquist-filter frequency response. Thus, the cascade of the modulator and demodulator produces a Nyquist-filter response which ideally exhibits zero ISI. In order to accommodate a variety of applications with different symbol rates and IF center frequencies, it is desirable for these filters to be programmable and as efficient as possible. We propose such a filtering system including, in particular, the method of designing the PSF.

## 2. CIC FILTER

The interpolation/decimation filter has a cascaded integrator comb (CIC) structure [1]. This is a very hardware-efficient way to construct a programmable interpolation/decimation filter since it does not involve the storing of filter coefficients or the use of costly multipliers. Fig. 2 shows a CIC interpolation filter, and Fig. 3 shows a CIC decimation filter. They consist of two main sections: the

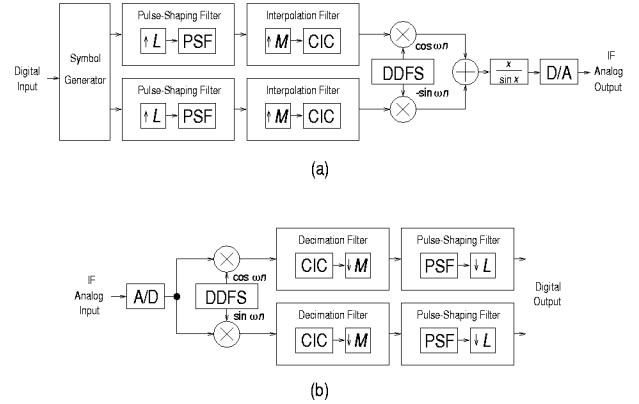


Fig. 1. (a) Modulator block diagram. (b) Demodulator filter block diagram.

cascade of  $P$  combs with the transfer function

$$H_C(z) = (1 - z^{-1})^P \quad (1)$$

and the cascade of  $P$  integrators with transfer function

$$H_I(z) = \left( \frac{1}{1 - z^{-1}} \right)^P. \quad (2)$$

They are separated by an expander/decimator of ratio  $M$ . After moving the expander/decimator through the combs/integrators by application of the noble identities [2], the CIC filter becomes a single lowpass filter with transfer function

$$H_{CIC}(z) = \left( \frac{1 - z^{-M}}{1 - z^{-1}} \right)^P = \left( \sum_{k=0}^{M-1} z^{-k} \right)^P \quad (3)$$

and frequency response

$$H_{CIC}(e^{j\omega}) = \left( \frac{\sin \frac{\omega M}{2}}{\sin \frac{\omega}{2}} e^{-j\omega \frac{M-1}{2}} \right)^P. \quad (4)$$

This linear-phase frequency response has a lowpass  $\frac{\sin Mx}{\sin x}$  characteristic with nulls at integer multiples of  $\frac{1}{M}F_s$ , where  $F_s$  is the higher sampling frequency. Thus, the images/aliases that result from the expansion/decimation are attenuated by this “natural” rejection. The location of the worst-case image/alias rejection and

This work was supported by the State of California MICRO Grant 97-207 and National Science Foundation Grant MIP-9632698.

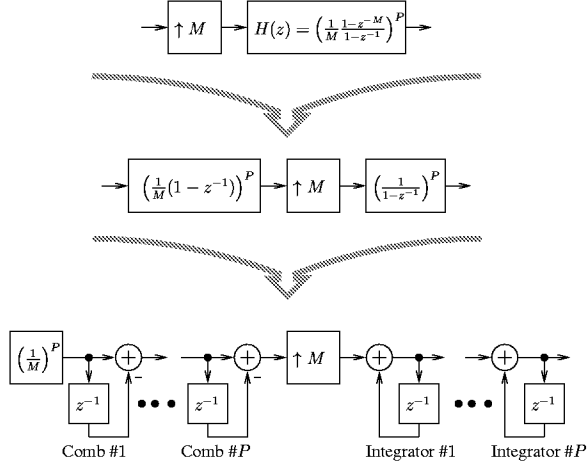


Fig. 2. CIC interpolation filter with DC gain normalization.

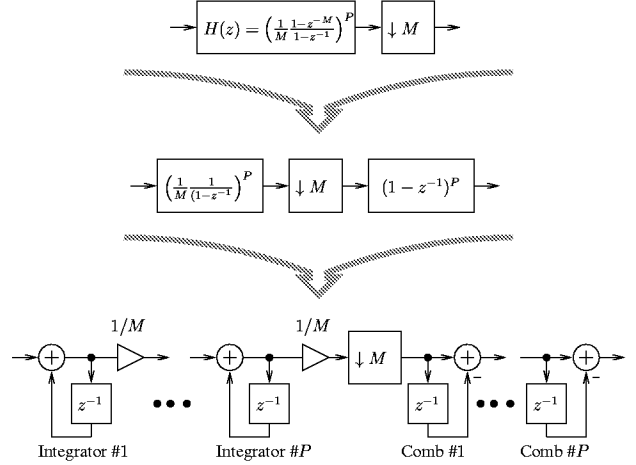


Fig. 3. CIC decimation filter with DC gain normalization.

the passband edge are determined by the rate change  $L$  of the preceding/following PSF. Normalized with respect to the high sampling rate  $F_s = 1$ , the passband edge is

$$f_C = \frac{\pi}{LM} \frac{1}{2\pi} = \frac{1}{2LM} \quad (5)$$

and the worst-case image/alias rejection occurs at

$$f_{AI} = \frac{1}{M} - f_C = \frac{2L-1}{2LM}. \quad (6)$$

Fig. 4 shows the “natural” rejection and the passband and imaging/aliasing bands for a single-stage ( $P = 1$ ) CIC filter with  $L = 4$ . The passband response suffers from droop which will cause ISI. Fig. 5 shows the worst-case passband droop and image/alias rejection as a function of the rate change  $M$  for a  $P$ -stage CIC filter with  $L = 4$ . Typical QAM systems require at least 45 dB of out-of-band attenuation, and at this amount of image/alias rejection, the amount of CIC-filter-induced ISI is more than can be tolerated. A sharpened CIC filter [3],[4] can be used to smooth out the passband, but this approach requires multiple copies of the

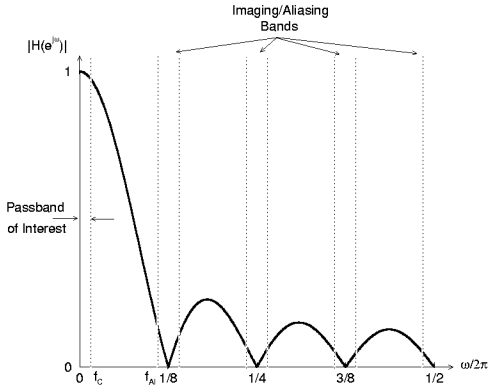


Fig. 4. Single-stage ( $P = 1$ ) CIC frequency response for  $M = 8$  with imaging/aliasing bands shown for  $L = 4$ .

basis filter. A more hardware-efficient way is to compensate for the passband droop by pre/post-distorting the signal in the preceding/following PSF. The CIC filter also has an intrinsic DC gain of  $M^P$ . The normalization of overall DC gain is achieved by using the method described in [4]. First, the DC gain is coarsely scaled by down-shifting the signal by  $K = \lceil \log_2 M^P \rceil$  bits. Then the gain is fine-tuned by programming the PSF to have a DC gain of  $\frac{2^K}{M^P}$ .

### 3. PSF

It is desirable for the PSF to have linear phase so roughly half of the coefficients need to be stored. In addition, the PSF must provide the required stopband attenuation for the system as well as a variable roll-off factor  $\alpha$  to accommodate different spectral shaping requirements. The PSF design is therefore a transmit-receive square-root Nyquist-filter design problem with the added constraint of passband droop compensation and gain adjustment. Of course, the linear-phase requirement of the PSF and the desire for the cascade of the PSF and CIC filter to exhibit zero ISI and a matched-filter response cannot all be met and therefore design

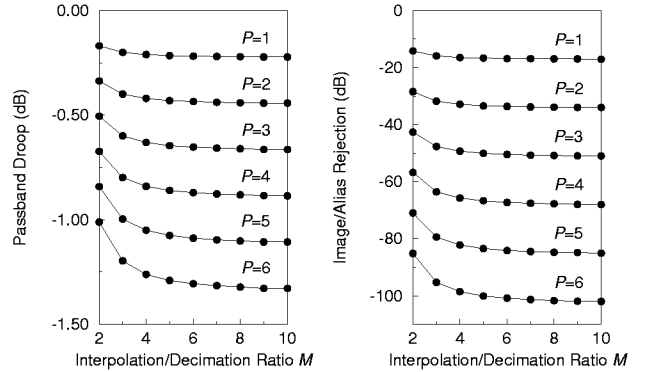


Fig. 5. Worst-case passband droop and image/alias rejection as a function of the rate change  $M$  for a  $P$ -stage CIC filter with  $L = 4$ .

decisions must be made. We have chosen to relax the zero ISI constraint and to design a PSF with linear phase whose cascade with the CIC filter exhibits a matched filter response with minimal ISI.

#### 4. PSF COEFFICIENT DESIGN ALGORITHM

A coefficient computation methodology has been developed to design filters which meet the above specifications. First, an appropriate length CIC filter is determined that will provide the necessary stopband attenuation for the image/alias with the desired interpolation/decimation ratio  $M$ . Next, an oversampled by  $L$  Nyquist filter is generated [5]-[7] which gives twice the desired out-of-band attenuation required by the modulator. Then, the square root of the Nyquist-filter frequency response is calculated. This is the target frequency response  $H_{TARGET}(e^{j\omega})$  for the cascade of the PSF, expander, and CIC filter in the modulator. The linear-phase coefficients of the PSF are then designed so that  $H_{TX}(e^{j\omega})$ , the frequency response of the cascaded PSF and CIC filter, is as close as possible to the target response. This is accomplished by using linear programming. If we let the PSF be an  $N$ -tap ( $N$  odd) linear-phase FIR filter, then its frequency response is given by

$$H_{PSF}(e^{j\omega}) = h_0 + \sum_{n=1}^{(N-1)/2} 2h_n \cos \omega n. \quad (7)$$

The frequency response of the CIC filter  $H_{CIC}(e^{j\omega})$  is given by (4). Therefore,

$$H_{TX}(e^{j\omega}) = H_{PSF}(e^{j\omega}) \uparrow_M H_{CIC}(e^{j\omega}) 2^{-K} \quad (8)$$

where  $\uparrow_M$  indicates the frequency compression by  $M$  of the expander and  $2^{-K}$  is the coarse DC gain normalization. The passband, transition band, and stopband of  $H_{TX}(e^{j\omega})$  are constrained to be as close as possible to the desired target  $H_{TARGET}(e^{j\omega})$ .

$$H_{TARGET}(e^{j\omega}) - \delta_i \leq H_{TX}(e^{j\omega}) \leq H_{TARGET}(e^{j\omega}) + \delta_i \quad (9)$$

where  $\delta_i$  is the band ripple. The above constraint is converted into linear programming problem format:

Minimize  $W_p \delta_p + W_s \delta_s + W_t \delta_t$  subject to

$$\left. \begin{aligned} H_{TX}(e^{j\omega}) - \delta_p &\leq H_{TARGET}(e^{j\omega}) \\ -H_{TX}(e^{j\omega}) - \delta_p &\leq -H_{TARGET}(e^{j\omega}) \end{aligned} \right\} 0 \leq \omega \leq \omega_p$$

$$\left. \begin{aligned} H_{TX}(e^{j\omega}) - \delta_t &\leq H_{TARGET}(e^{j\omega}) \\ -H_{TX}(e^{j\omega}) - \delta_t &\leq -H_{TARGET}(e^{j\omega}) \end{aligned} \right\} \omega_p < \omega < \omega_s$$

$$\left. \begin{aligned} H_{TX}(e^{j\omega}) - \delta_s &\leq H_{TARGET}(e^{j\omega}) \\ -H_{TX}(e^{j\omega}) - \delta_s &\leq -H_{TARGET}(e^{j\omega}) \end{aligned} \right\} \omega_s \leq \omega \leq \pi \quad (10)$$

where

$$\begin{aligned} W_p &= \text{passband weight}, & \delta_p &= \text{passband ripple}, \\ W_t &= \text{transition band weight}, & \delta_t &= \text{transition band ripple}, \\ W_s &= \text{stopband weight}, & \delta_s &= \text{stopband ripple}, \\ \omega_p &= \text{passband edge}, & & \\ \omega_s &= \text{stopband edge}. & & \end{aligned}$$

The full-precision coefficients obtained from the solution of the linear programming problem are then quantized to the desired number of bits by rounding followed by a bivariate local search [8]. Finally, the system is simulated with the designed filters, and the ISI signal-to-noise ratio (SNR) is calculated.

#### 5. RESULTS

Fig. 6 shows the filter design results for a 71-tap oversampled-by-four ( $L = 4$ ) PSF with  $\alpha = 0.25$  and 12-bit coefficients. The CIC filter has four stages ( $P = 4$ ) and the interpolation/decimation ratio  $M = 3$ . The frequency responses are normalized with respect to the high sampling rate  $F_s = 1$ . The CIC filter frequency response shows the coarse DC gain normalization, and the PSF frequency response shows the fine normalization. Since the maximum PSF coefficient magnitude [7] is  $1/L$  where  $L$  is greater than or equal to 2 and the maximum additional gain is less than or equal to 2, there is enough dynamic range to accommodate the fine gain adjustment without the need for increasing the coefficient wordlength. The additional gain automatically ends up in the PSF coefficients as the frequency response of the cascade of the PSF, expander, and CIC filter given by (8) is designed to be as close as possible to the target response which has unity gain. Table I lists the 12-bit PSF coefficients, and Fig. 7 shows the passband ripple for the cascade of the PSF and CIC filter and the target square-root Nyquist filter. The filters were simulated in the system of Fig. 1 resulting in an ISI SNR of 67 dB.

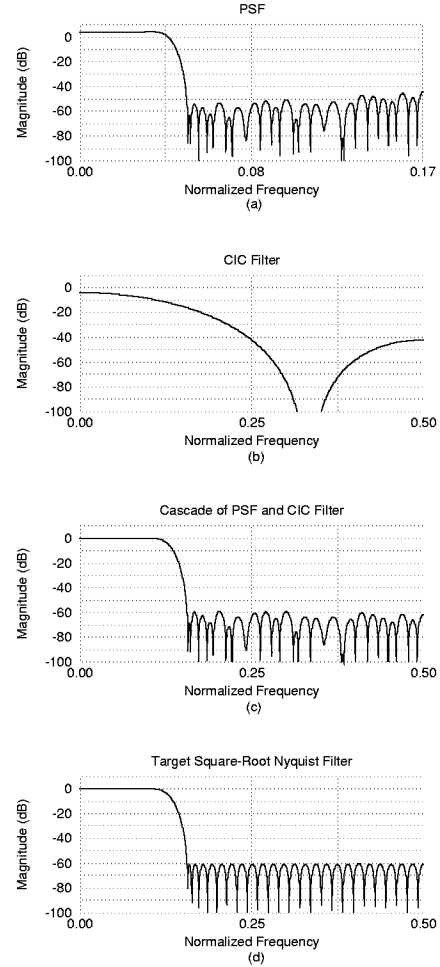


Fig. 6. Filter design results showing the frequency response of the (a) PSF, (b) CIC filter, (c) cascade of the PSF and CIC filter, and (d) the target square-root Nyquist filter normalized with respect to the high sampling rate  $F_s = 1$ .

TABLE I  
PSF COEFFICIENTS

Coefficient	Value
$h(0) = h(70) =$	-0.000976562500
$h(1) = h(69) =$	0.000488281250
$h(2) = h(68) =$	0.000488281250
$h(3) = h(67) =$	0.001464843750
$h(4) = h(66) =$	0.000488281250
$h(5) = h(65) =$	-0.000488281250
$h(6) = h(64) =$	-0.002441406250
$h(7) = h(63) =$	-0.002929687500
$h(8) = h(62) =$	-0.000976562500
$h(9) = h(61) =$	0.002441406250
$h(10) = h(60) =$	0.005371093750
$h(11) = h(59) =$	0.005371093750
$h(12) = h(58) =$	0.000976562500
$h(13) = h(57) =$	-0.005371093750
$h(14) = h(56) =$	-0.010253906250
$h(15) = h(55) =$	-0.008300781250
$h(16) = h(54) =$	0.000488281250
$h(17) = h(53) =$	0.011718750000
$h(18) = h(52) =$	0.017578125000
$h(19) = h(51) =$	0.011718750000
$h(20) = h(50) =$	-0.004394531250
$h(21) = h(49) =$	-0.022460937500
$h(22) = h(48) =$	-0.028808593750
$h(23) = h(47) =$	-0.015625000000
$h(24) = h(46) =$	0.013183593750
$h(25) = h(45) =$	0.041503906250
$h(26) = h(44) =$	0.047363281250
$h(27) = h(43) =$	0.019531250000
$h(28) = h(42) =$	-0.033203125000
$h(29) = h(41) =$	-0.082031250000
$h(30) = h(40) =$	-0.088867187500
$h(31) = h(39) =$	-0.026855468750
$h(32) = h(38) =$	0.099121093750
$h(33) = h(37) =$	0.253417968750
$h(34) = h(36) =$	0.379394531250
$h(35) =$	0.428222656250

## 6. CONCLUSION

The proposed variable-rate digital filtering system is hardware-efficient and the proposed coefficient design method provides a way to determine the PSF coefficients such that the cascade of the PSF and CIC filter produces the desired frequency response. The coefficient design algorithm works for all values of  $L$ ,  $M$ ,  $P$ ,  $N$ , and  $\alpha$ , and it produces a filter response that is close to the target response. The cascade of the modulator and demodulator filters produces an overall response that is close to a Nyquist-filter response with an acceptable amount of ISI for modern fixed-point digital communication systems. It is noted that the coefficient design method can be adapted to design the PSF when it is located in the demodulator and that the result is identical if the number of points in the frequency grid of (10) is consistent throughout the system of Fig. 1. It is also noted that mixed integer linear programming [9] can be used to determine the quantized coefficients of the

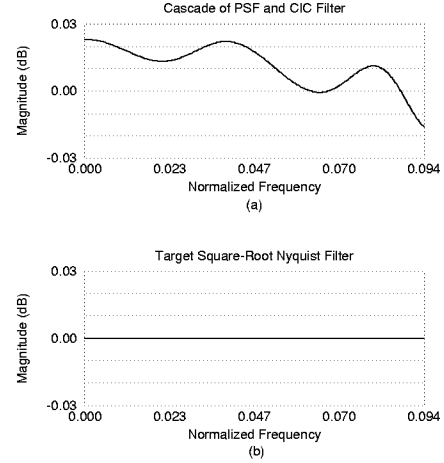


Fig. 7. Passband ripple for (a) the cascade of the PSF and CIC filter and (b) the target square-root Nyquist filter normalized with respect to the high sampling rate  $F_s = 1$ .

PSF instead of linear programming followed by a bivariate local search.

## 7. REFERENCES

- [1] E. B. Hogenauer, "An economical class of digital filters for decimation and interpolation," *IEEE Trans. Acoust., Speech, Signal Processing*, vol. ASSP-29, pp. 155–162, April 1981.
- [2] P. P. Vaidyanathan, *Multirate Systems and Filter Banks*. Englewood Cliffs, NJ: Prentice-Hall, 1993.
- [3] A. Y. Kwentus, Z. Jiang, and A. N. Willson Jr., "Application of filter sharpening to cascaded integrator-comb decimation filters," *IEEE Trans. Signal Processing*, vol. 45, pp. 457–467, Feb. 1997.
- [4] T.-C. Kuo, A. Y. Kwentus, and A. N. Willson Jr., "A programmable interpolation filter for digital communications applications," in *Proc. IEEE Int. Symp. Circuits Syst.*, Monterey, CA, June, 1998, vol. 2, pp. 97–100.
- [5] H. Samuelli, "On the design of optimal equiripple FIR digital filters for data transmission applications," *IEEE Trans. Circuits Syst.*, vol. 35, pp. 1542–1546, Dec. 1988.
- [6] H. Samuelli, "On the design of FIR digital data transmission filters with arbitrary magnitude specifications," *IEEE Trans. Circuits Syst.*, vol. 38, pp. 1563–1567, Dec. 1991.
- [7] F. Mintzer, "On half-band, third-band, and nth-band FIR filters and their design," *IEEE Trans. Acoust., Speech, Signal Processing*, vol. ASSP-30, pp. 734–738, Oct. 1982.
- [8] D. Kodek and K. Steiglitz, "Comparison of optimal and local search methods for designing finite wordlength FIR digital filters," *IEEE Trans. Circuits Syst.*, vol. CAS-28, pp. 28–32, Jan. 1981.
- [9] D. Kodek, "Design of optimal finite wordlength FIR digital filters using integer programming techniques," *IEEE Trans. Acoust., Speech, Signal Processing*, vol. ASSP-28, pp. 304–308, June 1980.